Centrality and system-size dependencies of temperatures of soft and hard components of p_t distributions of negative pions in ^{4}He + ^{12}C, ^{12}C + ^{12}C, and ^{12}C + ^{181}Ta collisions at $\sqrt{s_{NN}} = 3.14$ GeV

Kh. K. Olimov,[1,2,3,*] Akhtar Iqbal,[1] Mahnaz Q. Haseeb,[1] S. L. Lutpullaev,[2] and B. S. Yuldashev[4]

[1]*Department of Physics, COMSATS Institute of Information Technology, Park Road, 44000 Islamabad, Pakistan*

[2]*Physical-Technical Institute of SPA "Physics-Sun" of Uzbek Academy of Sciences, Bodomzor Yo'li str. 2[b], 100084 Tashkent, Uzbekistan*

[3]*Inha University in Tashkent, Ziyolilar str. 9, 100170 Tashkent, Uzbekistan*

[4]*Laboratory of High Energies, Joint Institute for Nuclear Research, RU-141980 Dubna, Russia*

(Received 4 March 2015; revised manuscript received 11 May 2015; published 18 August 2015)

Collision centrality as well as the system-size dependencies of the temperatures of the soft (p_t = 0.1−0.5 GeV/c) and hard (p_t = 0.5−1.2 GeV/c) components of the experimental transverse momentum distributions of the negative pions produced in ^{4}He+^{12}C, ^{12}C+^{12}C, and ^{12}C+^{181}Ta collisions at 4.2A GeV/c ($\sqrt{s_{NN}} = 3.14$ GeV) are analyzed. For the studied collision systems and selected collision centralities, the temperatures are extracted from fitting separately the soft and hard p_t components of the negative pions by one-temperature Hagedorn and one-temperature Boltzmann functions. The extracted temperatures of both the soft and hard components of the p_t distributions of π^- depend on the geometry (size) and degree of overlap of the colliding nuclei in peripheral, semicentral, and central nucleus–nucleus collisions at $\sqrt{s_{NN}} = 3.14$ GeV. The gap (differences) between the extracted temperatures in the studied collision systems increases with increasing the degree of overlap of the colliding nuclei, i.e., with an increase in the collision centrality and the corresponding increase in the numbers of participant nucleons and binary collisions. The temperature of the soft p_t component of the negative pions in ^{12}C+^{12}C (^{12}C+^{181}Ta) collisions increases (decreases) with increasing of the collision centrality. The temperature of the hard p_t component of π^- in ^{12}C+^{181}Ta (^{4}He+^{12}C) collisions increases (decreases) consistently with an increase in the collision centrality. The temperature of the soft p_t component of π^- decreases with an increase in the system size in semicentral and central nucleus–nucleus collisions at $\sqrt{s_{NN}} = 3.14$ GeV. In central collisions, the temperature of the hard p_t component increases consistently with an increase in system size. The physical interpretations of the results obtained are given. The quantitative results on temperatures extracted from the p_t spectra of negative pions in nucleus–nucleus collisions at 4.2A GeV/c are compared to those obtained in lower, intermediate, and higher energies in other Joint Institute for Nuclear Research (JINR), Gesellschaft für Schwerionenforschung (GSI), and SPS experiments.

DOI: 10.1103/PhysRevC.92.024909 PACS number(s): 14.40.Be, 25.10.+s, 25.70.Mn

I. INTRODUCTION

Pions are the predominantly produced particles in relativistic nuclear collisions due to the low threshold energies of their production in nucleon–nucleon collisions, which are around 290 and 280 MeV for charged and neutral pions, respectively [1]. The temperatures of pions, extracted from their transverse momentum or transverse mass (energy) distributions, are important for the analysis of the nuclear equation of state and for probing the freeze-out conditions after the expansion of a fireball, produced in central heavy ion collisions at high energies. In the past, pion production was suggested as a probe of compressional energy in the high-density phase of almost head-on collisions [2].

The excitation and decay of baryon resonances were shown to be one of the main mechanisms responsible for pion production in relativistic nuclear collisions. It was shown that a significant fraction of the pions produced in experiments on 2-m propane and 1-m hydrogen bubble chambers of the Joint Institute for Nuclear Research (JINR, Dubna, Russia) came from the decay of delta resonances [3–11]. The delta resonances played an important role in pion production and also in heavy ion collisions at the energies of the order of 1–10 GeV/nucleon [12–16]. As deduced from the analysis of relativistic heavy ion collisions [14], delta resonances were produced at the early "hot" compressional phase of a collision. At a later expansion phase, these resonances decay into nucleons and pions as the collision system gets cooled down significantly. The kinematics of Δ decay was shown to be responsible for the low transverse momentum enhancement of pion p_t distributions in hadron–nucleus and nucleus–nucleus collisions at incident beam energies from 1 to 15 GeV per nucleon [3,15,16].

The properties of the highly excited compressed nuclear matter (or those of a fireball at sufficiently high collision energies), created in central nucleus–nucleus collisions at relativistic energies, can be deduced from the analysis of the collision centrality and system-size dependencies of rapidity and transverse momentum distributions of pions [12,17–22]. The analysis of the pion rapidity distribution in Mg + Mg collisions at 4.3A GeV/c [22] showed that the central rapidity region was occupied with pions of significantly larger p_t as compared to the fragmentation region of colliding nuclei. The rapidity distributions of the negative pions in (p, d, α, C) + C and (d, α, C) + Ta collisions at 4.2A GeV/c were analyzed for

*olimov@comsats.edu.pk, drolimov@gmail.com

different transverse momentum ranges of π^- by the authors of Refs. [20,21]. As the transverse momentum of π^- increased, their fraction in the central rapidity region increased, and the corresponding fraction in the fragmentation region of colliding nuclei decreased. Negative pions with large p_t were mostly concentrated in the central rapidity range [20,21]. The quantitative analysis of the centrality dependence of rapidity as well as $\langle p_t \rangle$ versus the rapidity spectra of π^- mesons in $d + {}^{12}$C, ^{12}C+^{12}C, and ^{12}C+^{181}Ta collisions at 4.2A GeV/c was made in Ref. [23] by fitting the pion spectra with the Gaussian function. The widths of the rapidity distributions of π^- decreased in going from peripheral to central $d + {}^{12}$C, ^{12}C+^{12}C, and ^{12}C+^{181}Ta collisions [23]. With an increase in collision centrality, the centers of the rapidity distributions of the negative pions remained at the midrapidity position for symmetric ^{12}C+^{12}C collisions, whereas they shifted towards the target-fragmentation region in the case of asymmetric $d + {}^{12}$C and ^{12}C+^{181}Ta collisions. The extracted widths and locations of the centers of $\langle p_t \rangle$ versus the rapidity spectra of negative pions did not show, within the uncertainties, any dependence on the masses of projectile and target nuclei as well as the collision centrality [23]. The width of the rapidity distribution of particles, produced in relativistic nucleus–nucleus collisions, was deduced to carry information on the longitudinal flow [24] and final-state rescattering [25]. For a given freeze-out temperature, the width of the rapidity distribution was found to be sensitive to a velocity of sound in a medium at freeze-out in the Landau hydrodynamical model [26].

The temperatures of pions were estimated and studied for different sets of colliding nuclei at various energies in the past [27–36]. Transverse momentum and transverse mass distributions were preferred for extracting the hadron temperatures due to their Lorentz invariance with respect to longitudinal boosts [28,31,33,37]. The spectral temperatures of π^- mesons produced in $d + {}^{12}$C, ^{4}He+^{12}C, and ^{12}C+^{12}C collisions at 4.2A GeV/c were extracted by fitting noninvariant center-of-mass (c.m.) energy spectra of π^- mesons with the Maxwell-Boltzmann distribution function in Ref. [27]. The rapidity and angular dependencies of spectral temperatures of π^- mesons produced in ^{12}C+^{12}C collisions at 4.2A GeV/c were analyzed by the authors of Ref. [36]. The centrality and rapidity range dependencies of the shapes of the p_t distributions of the negative pions were studied separately in ^{12}C+^{12}C [34] and ^{12}C+^{181}Ta [35] collisions at 4.2A GeV/c. The transverse momentum as well as the energy spectra of pions, produced in relativistic hadron–nucleus and nucleus–nucleus collisions, demonstrated the two temperature shapes. The lower temperature (T_1) component was dominant contributing ∼(80–90)% to the total pion spectra, and the higher temperature (T_2) one accounted for the remaining ∼(10–20)% part [27,28,33–35,38]. However, practically no centrality dependence of these temperatures could be revealed from fitting the whole or main part of p_t and the c.m. energy distributions of pions in the past [27,33–35,38]. The reason for this could be the interplay of the temperatures of the soft and hard parts of the pion spectra while performing the combined two-temperature model fits. It is therefore of interest to study the centrality dependence of the shapes (temperatures) of the p_t distributions of pions, produced in relativistic nuclear collisions, separately in the soft and hard p_t regions.

This work is a further continuation of our recent papers [33–36] on the analysis of various features of pion spectra in nucleus–nucleus collisions at 4.2A GeV/c. The aim of the present paper is to study and reveal the centrality and system-size dependencies of the temperatures of the soft ($p_t = 0.1-0.5$ GeV/c) and hard ($p_t = 0.5 - 1.2$ GeV/c) parts of the experimental p_t distributions of the negative pions produced in ^{4}He+^{12}C, ^{12}C+^{12}C, and ^{12}C+^{181}Ta collisions at 4.2A GeV/c ($\sqrt{s_{NN}} = 3.14$ GeV). For these collision systems and the elected collision centralities, the temperatures will be extracted from fitting separately the soft and hard p_t components of π^- mesons by one-temperature Hagedorn as well as one-temperature Boltzmann functions. It is of interest to ascertain whether there is any observable dependence of the temperature of both the soft and hard p_t components of π^- on the size and degree of overlap of the colliding nuclei in peripheral, semicentral, and central nucleus–nucleus collisions at $\sqrt{s_{NN}} = 3.14$ GeV.

The paper is organized as follows. The experimental procedures are presented in Sec. II. The general kinematical characteristics of the negative pions and a brief overview of the two-temperature behavior of their p_t distributions in the studied collision systems are given in Sec. III. An analysis of the soft and hard components of p_t distributions of the negative pions and results are described in Sec. IV. Section V contains the summary and conclusions of the present work.

II. EXPERIMENT

The experimental data analyzed in the present work were obtained using a 2-m propane (C_3H_8) bubble chamber of the Laboratory of High Energies of JINR (Dubna, Russia). The 2-m propane bubble chamber was placed in a magnetic field of strength 1.5 T [19,27,39–41]. Three tantalum ^{181}Ta foils were also placed in the experimental setup of the chamber. The thickness of each foil was 1 mm, and the separation distance between foils was 93 mm. The bubble chamber was then irradiated with beams of ^{4}He and ^{12}C nuclei accelerated to a momentum of 4.2 GeV/c per nucleon at the Dubna synchrophasotron. The nuclei of ^{4}He and ^{12}C were made to interact with the carbon nuclei and protons of the propane molecules and the tantalum ^{181}Ta foils placed in the propane bubble chamber [19,27,39–41]. The methods of selection of inelastic ^{4}He+^{12}C, ^{12}C+^{12}C, and ^{12}C+^{181}Ta collision events in this experiment were explained in detail in Refs. [19,27,39–41]. The threshold for the detection and measurement of π^- mesons in the propane bubble chamber was ∼70 MeV/c for ^{4}He+^{12}C and ^{12}C+^{12}C collisions, whereas for ^{12}C+^{181}Ta collisions it was ∼80 MeV/c [19,27,39–41]. In some momentum and angular intervals, the particles could not be detected with 100% efficiency. To account for small losses of particles emitted under large angles to the object plane of the camera and due to tantalum foils, the relevant corrections were introduced as discussed by the authors of Refs. [19,27,39–41]. The average uncertainty in the measurement of the emission angle of negative pions was ∼0.8 degrees. The mean relative uncertainty of the momentum measurement of π^- mesons from the curvature of their tracks in the propane bubble chamber was ∼6%. All the negative

TABLE I. Mean multiplicities per event of the negative pions and participant protons and the average values of rapidity and transverse momentum of π^- mesons in ^{4}He+^{12}C, ^{12}C+^{12}C [23,34], and ^{12}C+^{181}Ta [23,35] collisions at 4.2A GeV/c per nucleon. The mean rapidities are calculated in the c.m. of nucleon–nucleon collisions at 4.2 GeV/c. Only statistical errors are given here and in the tables that follow.

Type		$\langle n(\pi^-)\rangle$	$\langle n_{\text{part.prot.}}\rangle$	$\langle y_{\text{c.m.}}(\pi^-)\rangle$	$\langle p_t(\pi^-)\rangle$ (GeV/c)
^{4}He + ^{12}C	Exper.	1.02 ± 0.01	2.83 ± 0.02	–0.090 ± 0.007	0.247 ± 0.002
	QGSM	0.99 ± 0.01	2.60 ± 0.01	–0.082 ± 0.007	0.224 ± 0.001
^{12}C+^{12}C	Exper.	1.45 ± 0.01	4.35 ± 0.02	–0.016 ± 0.005	0.242 ± 0.001
	QGSM	1.59 ± 0.01	4.00 ± 0.02	0.007 ± 0.005	0.219 ± 0.001
^{12}C+^{181}Ta	Exper.	3.50 ± 0.10	13.3 ± 0.2	–0.34 ± 0.01	0.217 ± 0.002
	QGSM	5.16 ± 0.09	14.4 ± 0.2	–0.38 ± 0.01	0.191 ± 0.001

particles, except the identified electrons, were considered to be π^- mesons. Admixtures of unidentified electrons and negative strange particles among them were less than 5% and 1%, respectively. In our experiment, the spectator protons are protons with momenta $p > 3$ GeV/c and the emission angle $\theta < 4$ degrees (projectile spectators), and protons with momenta $p < 0.3$ GeV/c (target spectators) [19,27,39–41]. Hence, the participant protons are those protons that remain after the elimination of spectator protons.

The statistics of the experimental data analyzed in the present work consist of 11974, 20528, and 2420 ^{4}He+^{12}C, ^{12}C+^{12}C, and ^{12}C+^{181}Ta minimum bias inelastic collision events, respectively, with practically all the secondary charged particles detected and measured with 4π acceptance.

III. GENERAL OVERVIEW

A comparison of the mean multiplicities per event of the negative pions and participant protons and the average values of rapidity and p_t of π^- mesons in minimum bias ^{4}He +C, ^{12}C+^{12}C [23,34], and ^{12}C+^{181}Ta [23,35] collisions at 4.2 GeV/c per nucleon both in the experiment and quark gluon string model (QGSM) is presented in Table I.

The QGSM was developed to describe hadron–nucleus and nucleus–nucleus collisions at high energies [42–45]. In the QGSM, hadron production occurs via formation and decay of quark-gluon strings. This model is used as a basic process for the generation of hadron–hadron collisions. In this model, nucleus–nucleus collisions are considered as a set of independent interactions of nucleons from projectile and target nuclei and of stable secondary hadrons and resonances. In the present work, the version of QGSM [43] adapted to the range of intermediate energies ($\sqrt{s_{NN}} \leqslant 4$ GeV) was used. The incident momentum of 4.2 GeV/c per nucleon for nucleus–nucleus collisions analyzed in the present work corresponds to incident kinetic energy 3.37 GeV per nucleon and nucleon–nucleon c.m. energy $\sqrt{s_{NN}} = 3.14$ GeV. The QGSM is based on Regge and string phenomenology of particle production in inelastic binary hadron collisions. To describe the evolution of the hadron and quark-gluon phases, a coupled system of Boltzmann-like kinetic equations is used in the model. The nuclear collisions are treated as a superposition of the independent interactions of the projectile and target nucleons, stable hadrons, and short-lived resonances. Resonant reactions like $\pi + N \to \Delta$, pion absorption by NN quasideuteron pairs, and also $\pi + \pi \to \rho$ reactions were taken into account in the model. The time of the formation of hadrons was also included in QGSM. The masses of strings at intermediate energies are very small. At $\sqrt{s_{NN}} = 3.14$ GeV the masses of strings are smaller than 2 GeV, and these strings fragment predominantly (∼90%) through the two-particle decay channel. In the QGSM, Δ^0 and Δ^- resonances and ρ^-, ρ^0, ω, η, and η' as well as the so-called "prompt" π^- mesons are sources of the negative pions. "Prompt" π^- mesons are produced directly in hadron–hadron collisions. These can be primary or secondary NN collisions ($NN \to NN\pi$), or interactions of secondary mesons with nucleons ($\rho N \to \pi N$). The decay of excited recoil nuclear fragments and a coupling of nucleons inside the nucleus were not taken into account in QGSM. To simulate real experimental conditions, the QGSM events were passed through a "filter." As a result of this filtering procedure, all the slow particles absorbed in the 2-mm propane layer and in tantalum foils were excluded. A more detailed description of QGSM is given in Refs. [42–45].

As seen from Table I, on the whole, the QGSM describes qualitatively all the average characteristics of the negative pions in the experiment except for the mean multiplicity of π^- mesons in ^{12}C+^{181}Ta collisions and their $< p_t >$ in all three collisions' systems. The QGSM overestimates significantly the multiplicity of π^- in ^{12}C+^{181}Ta collisions at 4.2A GeV/c. This can be explained by the fact that the QGSM simplifies the nuclear effects, which are more pronounced in heavy nuclei [46,47]. It was suggested by the authors of Ref. [47] that this model can be improved by taking into account a possible increase of the pion absorption cross section in the dense baryon medium, as well as by including the higher mass baryon resonances. As observed from Table I, QGSM underestimates noticeably the average values of p_t of the negative pions in all three collisions systems. The experimental transverse momentum and rapidity distributions of π^- along with the corresponding QGSM spectra in minimum bias ^{4}He +C, ^{12}C+^{12}C, and ^{12}C+^{181}Ta collisions at 4.2A GeV/c are presented in Fig. 1. Figure 1(a) shows that the QGSM underestimates the experimental p_t spectrum of π^- mesons in the region $p_t > 0.8$ GeV/c. It is worth mentioning that another model − the modified FRITIOF model [48–51], specifically modified for describing the nucleus–nucleus collisions at incident energies of the order of a few GeV per nucleon, also underestimates this high p_t part of the pion spectra [33,52]. As observed from Fig. 1(b), the QGSM describes satisfactorily

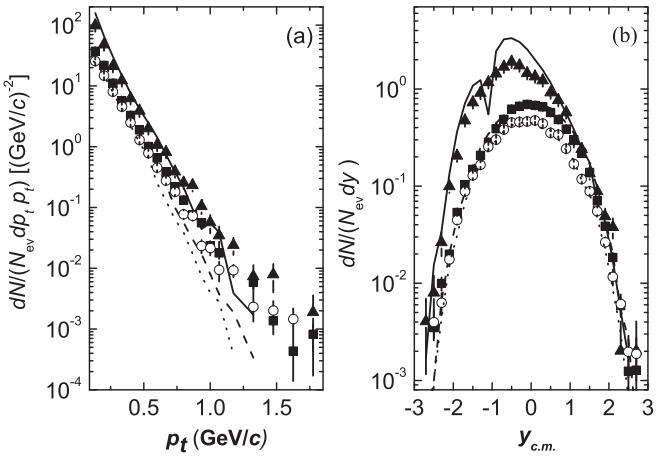

FIG. 1. (a) The experimental transverse momentum and (b) rapidity distributions of the negative pions produced in minimum bias ^{4}He+^{12}C (○), ^{12}C+^{12}C [34] (■), and ^{12}C+^{181}Ta [35] (▲) collisions at 4.2 GeV/c per nucleon. The rapidity distributions were plotted in the c.m. of nucleon–nucleon collisions at 4.2 GeV/c. The corresponding calculated QGSM spectra are given by the dotted (^{4}He+^{12}C), dashed (^{12}C+^{12}C), and solid (^{12}C+^{181}Ta) curves. All the spectra are normalized per one inelastic collision event.

the experimental rapidity distributions in the studied collision systems.

However, as can be seen from Fig. 1(b), the double peak structure with a dip at $y_{\text{c.m.}} \approx -1$ is observed in the QGSM rapidity distribution of the negative pions in ^{12}C+^{181}Ta collisions. The appearance of this structure in the model is likely due to the separation of the heavy target fragmentation region from the central rapidity region in ^{12}C+^{181}Ta collisions, whereas the central rapidity and projectile fragmentation regions overlap with each other due to their relative closeness in the rapidity space [35]. The absence of such a structure in the experimental rapidity distribution is likely due to the experimental broadening caused by the experimental resolution of the spectrum. Hence, the target fragmentation and central rapidity regions overlap in the experimental rapidity distribution of the negative pions.

In Refs. [34,35] the p_t distributions of the negative pions, produced in ^{12}C+^{12}C and ^{12}C+^{181}Ta collisions at 4.2A GeV/c, were described successfully by the Boltzmann and Hagedorn thermodynamic model functions. The Hagedorn thermodynamic model [37,53] allows for a set of fireballs displaced from each other in rapidity. In this model, particles with different momenta freeze-out within a volume that is of universal magnitude when assessed in the rest frame for any given momentum, being the distribution in the transverse momentum of the shape $dN/d\,p_t = \text{const} \cdot p_t \cdot m_t \cdot K_1(m_t/T) \approx \text{const} \cdot p_t \cdot (m_t \cdot T)^{1/2} \cdot \exp(-m_t/T)$, where K_1 is the MacDonald function, $m_t = \sqrt{m^2 + p_t^2}$ is the transverse mass, and T is the temperature. The above approximation is valid for $m_t \gg T$. Hence, the Hagedorn thermodynamic model [37,53] predicts that the normalized transverse momentum distribution of hadrons can be described using the expression (assuming $m_t \gg T$)

$$\frac{dN}{N\,p_t d\,p_t} = A \cdot (m_t T)^{1/2} \exp\left(-\frac{m_t}{T}\right), \tag{1}$$

where N (depending on the choice of normalization) is either the total number of inelastic collision events or the total number of the respective hadrons, and A is the fitting constant. This relation (1) will be referred to as the one-temperature Hagedorn function throughout the present work. Correspondingly, in the case of two temperatures T_1 and T_2, the above formula is modified as

$$\frac{dN}{N\,p_t d\,p_t} = A_1 \cdot (m_t T_1)^{1/2} \exp\left(-\frac{m_t}{T_1}\right) + A_2 \cdot (m_t T_2)^{1/2} \exp\left(-\frac{m_t}{T_2}\right), \tag{2}$$

referred to as the two-temperature Hagedorn function.

The Boltzmann model assumes that the transverse momentum distributions of hadrons can be described using the m_t Boltzmann distribution function given by

$$\frac{dN}{N\,p_t d\,p_t} = A\,m_t \exp\left(-\frac{m_t}{T}\right), \tag{3}$$

referred to as the one-temperature Boltzmann function in the present paper. In the case of two temperatures T_1 and T_2, the above formula is modified as

$$\frac{dN}{N\,p_t d\,p_t} = A_1 \cdot m_t \exp\left(-\frac{m_t}{T_1}\right) + A_2 \cdot m_t \exp\left(-\frac{m_t}{T_2}\right). \tag{4}$$

To analyze quantitatively the change in the shape of p_t distributions of the negative pions in ^{12}C+^{12}C [34] and ^{12}C+^{181}Ta [35] collisions with an increase in collision centrality (which corresponds to a decrease of the impact parameter of the collision), the number of participant protons (N_P) was used to characterize the collision centrality. References [19,34,35,54] were followed to define the peripheral collision events to be those in which $N_p \leqslant \langle n_{\text{part.prot}} \rangle$, and the central collisions as the collision events with $N_p \geqslant 2\langle n_{\text{part.prot}} \rangle$, where $\langle n_{\text{part.prot}} \rangle$ is the mean multiplicity per event of participant protons, and the semicentral collisions come in between these two multiplicity regions. It was shown in Ref. [54] that the central ^{12}C+^{12}C collisions at 4.2A GeV/c selected using the above criterion were characterized by complete projectile stopping because in these collisions the average number of interacting projectile nucleons (the average number of participant nucleons from the projectile nucleus) was very close to the total number of nucleons in projectile carbon. Fractions of central, semicentral, and peripheral ^{4}He +C, ^{12}C+^{12}C [23,34], and ^{12}C+^{181}Ta [23,35] collision events, relative to the total inelastic cross section, obtained for both experimental and QGSM data, are presented in Table II. As seen from Table II, on the whole, the experimental fractions of peripheral, semicentral, and central ^{4}He +C, ^{12}C+^{12}C, and ^{12}C+^{181}Ta collision events are reproduced quite satisfactorily by the QGSM calculations. Table II shows that the selected central collision events correspond to ∼(0–10)% centrality in ^{4}He +C and ^{12}C+^{12}C collisions and to ∼(0–15)% centrality in ^{12}C+^{181}Ta collisions.

TABLE II. Fractions of peripheral, semicentral, and central ^{4}He+^{12}C, ^{12}C+^{12}C [23,34], and ^{12}C+^{181}Ta [23,35] collisions at 4.2A GeV/c per nucleon, relative to the total inelastic cross section.

Type	Peripheral collisions (%)		Semicentral collisions (%)		Central collisions (%)	
	Experiment	QGSM	Experiment	QGSM	Experiment	QGSM
^{4}He+^{12}C	54 ± 1	54 ± 1	37 ± 1	38 ± 1	9 ± 1	8 ± 1
^{12}C+^{12}C	58 ± 1	62 ± 1	31 ± 1	30 ± 1	11 ± 1	8 ± 1
^{12}C+^{181}Ta	60 ± 2	56 ± 1	24 ± 1	29 ± 1	16 ± 1	15 ± 1

Table III presents the spectral temperatures of the negative pions in minimum bias ^{4}He+^{12}C, ^{12}C+^{12}C [34], and ^{12}C+^{181}Ta [35] collisions at 4.2A GeV/c and their relative contributions (R_1 and R_2) extracted from fitting their transverse momentum spectra in the whole p_t range by two-temperature Hagedorn and Boltzmann functions. They were compared to the corresponding results obtained by the authors of Ref. [27] from fitting the noninvariant c.m. energy spectra of the negative pions in the studied collisions at the same initial momentum (on about two times lesser statistics of collision events) using the two-temperature Maxwell-Boltzmann distribution function. The relative contributions of these two temperatures to the total negative pion multiplicity were calculated [34,35] over the total transverse momentum interval ($R_i = c_i/(c_1 + c_2)$, where $c_i = A_i \cdot \int (m_t T_i)^{1/2} \exp(-\frac{m_t}{T_i}) d p_t$ and $c_i = A_i \cdot \int m_t \exp(-\frac{m_t}{T_i}) d p_t$ ($i = 1, 2$) are for the case of Hagedorn and Boltzmann function fits, respectively). It is necessary to note that the R^2 factor in Table III is defined as $R^2 = 1 - \frac{SS_E}{SS_T}$, where $SS_E = \sum_{i=1}^{n} (y_i^{\exp} - y_i^{fit})^2$ is the total sum of the squares of the differences between the experimental and fit (model) data, $SS_T = \sum_{i=1}^{n} (y_i^{\exp} - \langle y \rangle)^2$ is the total sum of the squares of the deviations of the experimental data from their mean value, $y_i^{\exp}$ and y_i^{fit} are the original (experimental) and fit (model) data, respectively, and $\langle y \rangle = \frac{1}{n} \sum_{i=1}^{n} y_i^{\exp}$ is the mean value of the experimental data. As the deviation of the experimental data from the fit (model) data gets smaller, the R^2 factor approaches 1. Thus, the closer the R^2 factor value to 1, the better is the fit quality.

As seen from Table III, the values of the temperatures (T_1, T_2) extracted from fitting the p_t spectra by two-temperature Hagedorn and two-temperature Boltzmann functions proved to be noticeably lower [34,35] compared to the corresponding values, obtained [27] from fitting the noninvariant c.m. energy spectra of the negative pions by Maxwell-Boltzmann distribution function. This was likely due to the influence of longitudinal motion on the energy spectra of π^- mesons, in contrast to their p_t spectra, which are Lorentz invariant with respect to longitudinal boosts [28,31,33,37]. As observed from Table III, the dominant contribution ($R_1 \sim 80$–90%) to the total π^- multiplicity in the studied collision systems was given by T_1, which was compatible within the uncertainties with the results found in Ref. [27]. The fits by the Boltzmann function resulted in slightly lower values of the temperatures compared to those by the Hagedorn function [34,35].

Figure 2 shows, as an example, the experimental p_t distributions of π^- mesons produced in minimum bias ^{12}C+^{12}C [34] and ^{12}C+^{181}Ta [35] collisions at 4.2 GeV/c per nucleon along with the corresponding fits in the whole p_t range by one-temperature and two-temperature Hagedorn functions. It was concluded earlier [27,33–35,38], which can also be seen from Fig. 2, that the p_t as well as noninvariant c.m. energy distributions of the negative pions in minimum bias ^{4}He+^{12}C, ^{12}C+^{12}C, and ^{12}C+^{181}Ta collisions at 4.2A GeV/c exhibit two-temperature shapes.

The two-temperature shape of the pion spectra was observed also in other experiments in relativistic collisions of different sets of nuclei at various energies in the past [28–31]. In an earlier paper [28], the two-temperature shape of c.m.

TABLE III. Spectral temperatures (T) of the negative pions in minimum bias ^{4}He+^{12}C, ^{12}C+^{12}C [34], and ^{12}C+^{181}Ta [35] collisions at 4.2A GeV/c and their relative contributions (R_1 and R_2) extracted from fitting their experimental transverse momentum distributions in the whole p_t range by two-temperature Hagedorn and Boltzmann functions compared to the corresponding values obtained in Ref. [27] from fitting the noninvariant c.m. energy spectra of the negative pions by Maxwell-Boltzmann distribution function. (*n.d.f.* denotes the number of degrees of freedom)

Fitting Function	Collision Type	T_1 (MeV)	R_1 (%)	T_2 (MeV)	R_2 (%)	$\chi 2$/*n.d.f.*	R^2 factor
Hagedorn	HeC	83 ± 4	89 ± 14	150 ± 15	11 ± 8	1.43	0.99
	CC	76 ± 3	85 ± 14	142 ± 7	15 ± 6	1.32	0.99
	CTa	57 ± 3	80 ± 22	128 ± 6	20 ± 7	0.92	0.99
Boltzmann	HeC	68 ± 3	85 ± 13	124 ± 8	15 ± 7	1.44	0.99
	CC	65 ± 2	85 ± 13	127 ± 5	15 ± 4	1.40	0.99
	CTa	50 ± 2	83 ± 20	116 ± 5	17 ± 5	1.02	0.99
Maxwell-Boltzmann	HeC	94 ± 6	85 ± 11	173 ± 22	15 ± 11	0.54	–
	CC	83 ± 3	79 ± 6	145 ± 7	21 ± 6	0.72	–
	CTa	66 ± 2	88 ± 3	159 ± 6	12 ± 3	0.58	–

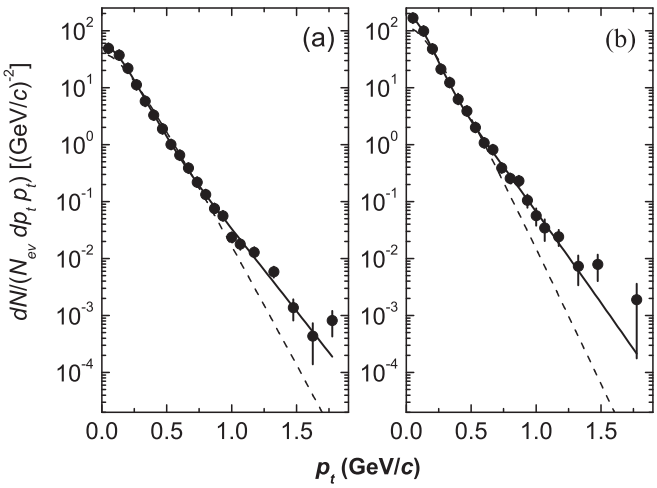

FIG. 2. (a) The experimental transverse momentum spectra (•) of the negative pions produced in minimum bias ^{12}C+^{12}C [34] and (b) ^{12}C+^{181}Ta [35] collisions at 4.2 GeV/c per nucleon and the corresponding fits in the whole p_t range by one-temperature (dashed lines) and two-temperature (solid lines) Hagedorn functions. All the spectra are normalized per one inelastic collision event.

kinetic energy spectra of the negative pions in Ar + KCl collisions at 1.8 GeV/nucleon was obtained. In this work, the occurrence of two temperatures T_1 and T_2 was interpreted as due to two channels of pion production: pions coming from Δ resonance decay (T_1), and directly produced pions (T_2). In Ref. [30] the two-temperature shape of the kinetic energy spectrum of pions emitted at 90º in c.m. of central La + La collisions at 1.35 GeV/nucleon was interpreted as due to different contributions of deltas originated from the earlier and later stages of heavy ion reactions. The two-temperature behavior was observed also for c.m. energy as well as the p_t spectra of π^- mesons produced in Mg + Mg collisions [31] at incident momenta of $4.2-4.3A$ GeV/c. It would be oversimplified to believe that the origin of pions in minimum bias nucleus–nucleus collisions could only be described by two thermal sources. The phenomenon of collective flow has become the well-established and important feature of relativistic heavy ion collisions. The inverse slope parameter T, or an apparent temperature of the emitting source, of the transverse mass spectra of hadrons was shown to consist of two components: a thermal part (T_{thermal}), and a second part resembling the collective expansion with an average transverse velocity $\langle\beta_t\rangle$ [55]. It is necessary to mention that the collective flow of protons and negative pions was observed experimentally also in He + C, C + C, C + Ne, C + Cu, and C + Ta collisions within the momentum range of $4.2-4.5A$ GeV/c [56–58]. The two-temperature shape of the pion spectra could also be explained qualitatively as due to two pion types: pions, emitted from the "hot" core of the collision zone at the initial collision stage, and other pions, coming later from the expansion and freeze-out of a highly compressed nuclear matter, or a fireball, created in central or semicentral nucleus–nucleus collisions. The low temperature part of the pion spectra can also be thought of as due to the contribution of a mixture of pions, originating from the expansion and freeze-out of a fireball, with "cold" pions coming from the decay of resonances at a later stage of the collision. In addition, the high temperature part of the spectra can certainly be due to pions produced in semi(hard) nucleon–nucleon collisions.

Hence, the observed two-temperature shape of the p_t distribution of pions, produced in minimum bias nucleus–nucleus collisions at $4.2A$ GeV/c, is likely to be due to the contribution of the combination of pions coming from collective flow, pions generated from the decay of various resonances, and pions produced in semi(hard) nucleon–nucleon collisions. Each of the above plausible sources should contribute to pion p_t distribution with a certain weight, which is expected to depend on collision centrality as well as the mass numbers and geometry of the colliding nuclei.

It is evident from Figs. 1 and 2 that the p_t spectra of the negative pions with $p_t \leqslant 1.2$ GeV/c are characterized by a good enough statistics of π^- and, therefore, by sufficiently low statistical errors. However, as seen from Figs. 1 and 2, the $p_t > 1.2$ range displays quite poor statistics of the produced pions and, hence, quite large statistical uncertainties. Due to the lower momentum threshold of the detection of pions $p_{\mathrm{thresh}} \approx 70-80$ MeV/c, it was natural [34,35] to fit the p_t distributions of pions in the range $p_t = 0.1-1.2$ GeV/c, where they were detected and measured with practically 100% efficiency.

Table IV presents the spectral temperatures of the negative pions in minimum bias ^{4}He+^{12}C, ^{12}C+^{12}C [34], and ^{12}C+^{181}Ta [35] collisions at $4.2A$ GeV/c and their relative contributions extracted from fitting their experimental p_t distributions in the range $p_t = 0.1-1.2$ GeV/c by two-temperature Hagedorn and Boltzmann functions. Figure 3 shows, as an example, the experimental transverse momentum distributions of the negative pions produced in minimum bias ^{12}C+^{12}C [34] and ^{12}C+^{181}Ta [35] collisions at 4.2 GeV/c per

TABLE IV. Spectral temperatures (T) of the negative pions in minimum bias ^{4}He+^{12}C, ^{12}C+^{12}C [34], and ^{12}C+^{181}Ta [35] collisions at $4.2A$ GeV/c and their relative contributions (R_1 and R_2) extracted from fitting their experimental transverse momentum distributions in range $p_t = 0.1-1.2$ GeV/c by two-temperature Hagedorn and Boltzmann functions.

Fitting function	Collision Type	T_1 (MeV)	R_1 (%)	T_2 (MeV)	R_2 (%)	χ^2/n.d.f.	R^2 factor
Hagedorn	HeC	67 ± 8	70 ± 30	122 ± 8	30 ± 18	1.15	0.99
	CC	59 ± 6	68 ± 33	119 ± 5	32 ± 14	0.44	0.99
	CTa	53 ± 5	77 ± 40	123 ± 6	23 ± 11	0.91	0.99
Boltzmann	HeC	59 ± 5	75 ± 26	112 ± 6	25 ± 12	1.17	0.99
	CC	54 ± 4	74 ± 27	111 ± 4	26 ± 9	0.42	0.99
	CTa	49 ± 3	81 ± 34	113 ± 5	19 ± 8	1.02	0.99

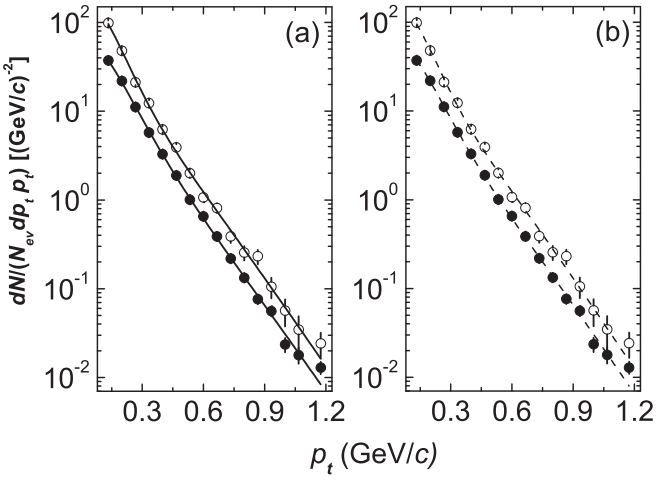

FIG. 3. The experimental transverse momentum spectra of the negative pions produced in minimum bias ^{12}C+^{12}C [34] (•) and ^{12}C+^{181}Ta [35] (○) collisions at 4.2 GeV/c per nucleon and the corresponding fits in range $p_t = 0.1-1.2$ GeV/c by (a) two-temperature Hagedorn (solid lines) and (b) two-temperature Boltzmann (dashed lines) functions. All the spectra are normalized per one inelastic collision event.

nucleon and the corresponding fits in the range $p_t = 0.1-1.2$ GeV/c by two-temperature Hagedorn and two-temperature Boltzmann functions. As seen from Fig. 3 and Table IV, the experimental p_t distributions of π^- exhibited two temperature shapes, being described quite well by two-temperature Hagedorn and Boltzmann functions in minimum bias ^{4}He+^{12}C, ^{12}C+^{12}C [34], and ^{12}C+^{181}Ta [35] collisions at 4.2 GeV/c per nucleon. As seen from Table IV, the lower temperature T_1 part dominates the p_t distributions of π^- mesons in the range $p_t = 0.1-1.2$ GeV/c, as was also the case for the whole p_t range. Spectral temperatures of π^- in peripheral, semicentral, and central ^{4}He+^{12}C, ^{12}C+^{12}C [34], and ^{12}C+^{181}Ta [35] collisions at 4.2A GeV/c and their relative contributions, extracted from fitting their experimental transverse momentum spectra in the range $p_t = 0.1-1.2$ GeV/c by two-temperature Hagedorn and Boltzmann functions, are presented in Table V. As seen from Table V, practically no centrality dependence of the extracted temperatures T_1 and T_2 was observed, which is likely due to the interplay between the temperatures of soft and hard components of pion p_t spectra while performing combined two temperature model fits, and partly due to significant fitting errors of T_1 and T_2. We, therefore, studied the centrality as well as system-size dependencies of the shapes (temperatures) of p_t distributions of π^- mesons by fitting separately their soft ($p_t = 0.1-0.5$ GeV/c) and hard ($p_t = 0.5-1.2$ GeV/c) p_t components by one-temperature Hagedorn and one-temperature Boltzmann functions in the present work.

IV. ANALYSIS AND RESULTS

Table VI presents the parameters extracted from fitting by one-temperature Hagedorn and one-temperature Boltzmann functions of the experimental p_t distributions of the negative pions in peripheral, semicentral, and central ^{4}He+^{12}C, ^{12}C+^{12}C, and ^{12}C+^{181}Ta collisions at 4.2A GeV/c in the fitting ranges $p_t = 0.1-0.5$ GeV/c and $p_t = 0.5-1.2$ GeV/c. As can be seen from a comparison of Tables V and VI, the separate fitting of the soft (0.1–0.5 GeV/c) and hard (0.5–1.2 GeV/c) p_t components of the negative pions resulted in significantly lower fitting uncertainties of the extracted temperatures as compared to the combined two-temperature

TABLE V. Spectral temperatures (T) of the negative pions in peripheral, semicentral, and central ^{4}He+^{12}C, ^{12}C+^{12}C [34], and ^{12}C+^{181}Ta [35] collisions at 4.2A GeV/c and their relative contributions (R_1 and R_2) extracted from fitting their experimental transverse momentum distributions in range $p_t = 0.1-1.2$ GeV/c by two-temperature Hagedorn and Boltzmann functions.

Fitting function	Centrality Type	Collision Type	T_1 (MeV)	R_1 (%)	T_2 (MeV)	R_2 (%)	χ^2/n.d.f.	R^2 factor
Hagedorn	Peripheral	HeC	67 ± 8	77 ± 35	125 ± 12	23 ± 19	0.99	0.99
		CC	62 ± 6	74 ± 34	123 ± 8	26 ± 15	0.73	0.99
		CTa	63 ± 7	83 ± 43	139 ± 16	17 ± 14	0.85	0.99
	Semicentral	HeC	57 ± 11	54 ± 45	112 ± 6	46 ± 32	1.53	0.99
		CC	60 ± 6	70 ± 33	123 ± 6	30 ± 14	0.27	0.99
		CTa	46 ± 7	70 ± 69	112 ± 6	30 ± 24	0.50	0.99
	Central	HeC	59 ± 20	48 ± 58	109 ± 10	52 ± 55	0.97	0.99
		CC	65 ± 8	70 ± 33	124 ± 8	30 ± 18	1.42	0.99
		CTa	49 ± 6	78 ± 58	119 ± 8	22 ± 15	1.11	0.98
Boltzmann	Peripheral	HeC	60 ± 5	81 ± 30	115 ± 9	19 ± 12	0.95	0.99
		CC	55 ± 4	78 ± 29	112 ± 6	22 ± 10	0.76	0.99
		CTa	56 ± 5	85 ± 39	123 ± 12	15 ± 10	0.93	0.98
	Semicentral	HeC	53 ± 7	65 ± 37	104 ± 5	35 ± 19	1.52	0.99
		CC	55 ± 4	77 ± 28	113 ± 5	23 ± 9	0.31	0.99
		CTa	44 ± 5	76 ± 57	104 ± 5	24 ± 15	0.49	0.99
	Central	HeC	54 ± 11	60 ± 50	100 ± 8	40 ± 32	0.98	0.99
		CC	58 ± 5	76 ± 28	114 ± 6	24 ± 12	1.40	0.99
		CTa	46 ± 4	82 ± 50	109 ± 7	18 ± 10	1.17	0.98

TABLE VI. Parameters extracted from fitting by one-temperature Hagedorn and one-temperature Boltzmann functions of the experimental transverse momentum distributions of the negative pions in peripheral, semicentral, and central ^{4}He+^{12}C, ^{12}C+^{12}C, and ^{12}C+^{181}Ta collisions at 4.2A GeV/c in the fitting ranges $p_t = 0.1-0.5$ GeV/c and $p_t = 0.5-1.2$ GeV/c.

Type			Fitting Range							
			$p_t = 0.1-0.5$ GeV/c				$p_t = 0.5-1.2$ GeV/c			
Fit. funct.	Centr. Type	Coll. Type	A	T (MeV)	χ^2/n.d.f.	R^2	A	T (MeV)	χ^2/n.d.f.	R^2
Hag.	Periph.	HeC	1173 ± 148	83 ± 2	0.36	0.99	140 ± 47	120 ± 6	0.97	0.96
		CC	1467 ± 170	81 ± 2	1.59	0.99	210 ± 57	116 ± 5	1.08	0.97
		CTa	2894 ± 474	81 ± 3	3.41	0.96	249 ± 72	113 ± 5	0.57	0.99
	Semicen.	HeC	2207 ± 267	87 ± 2	0.85	0.99	657 ± 194	110 ± 5	2.22	0.94
		CC	3819 ± 431	84 ± 2	2.73	0.98	573 ± 121	120 ± 4	0.28	0.99
		CTa	13710 ± 2179	76 ± 3	1.90	0.98	624 ± 144	118 ± 4	0.19	0.99
	Centr.	HeC	3908 ± 563	87 ± 3	0.44	0.99	2506 ± 1229	98 ± 7	0.93	0.95
		CC	6230 ± 738	86 ± 2	1.05	0.99	1023 ± 256	119 ± 5	1.88	0.96
		CTa	20167 ± 3589	75 ± 3	5.06	0.93	980 ± 428	128 ± 9	0.71	0.95
Bolt.	Periph.	HeC	1019 ± 116	74 ± 2	0.78	0.99	93 ± 29	111 ± 5	0.91	0.96
		CC	1258 ± 133	72 ± 2	2.51	0.98	140 ± 35	108 ± 4	1.14	0.97
		CTa	2496 ± 372	72 ± 2	4.30	0.95	164 ± 44	105 ± 4	0.58	0.99
	Semicen.	HeC	1951 ± 213	76 ± 2	1.55	0.99	423 ± 117	102 ± 4	2.22	0.94
		CC	3315 ± 341	74 ± 2	3.95	0.97	381 ± 76	111 ± 3	0.35	0.99
		CTa	11373 ± 1654	68 ± 2	2.63	0.97	417 ± 90	109 ± 4	0.22	0.99
	Centr.	HeC	3449 ± 448	76 ± 2	0.67	0.99	1575 ± 729	92 ± 6	0.97	0.95
		CC	5482 ± 589	75 ± 2	1.77	0.99	683 ± 160	110 ± 4	1.87	0.96
		CTa	16722 ± 2730	67 ± 2	6.09	0.92	670 ± 272	118 ± 8	0.71	0.95

fits in the range $p_t = 0.1-1.2$ GeV/c. Soft components of the experimental p_t distributions of the negative pions in peripheral, semicentral, and central ^{4}He+^{12}C, ^{12}C+^{12}C, and ^{12}C+^{181}Ta collisions at 4.2A GeV/c along with the corresponding fits by the one-temperature Hagedorn function in the p_t range $0.1 - 0.5$ GeV/c are presented in Fig. 4. Figure 5 presents hard components of the experimental p_t distributions of the negative pions in peripheral, semicentral, and central ^{4}He+^{12}C, ^{12}C+^{12}C, and ^{12}C+^{181}Ta collisions at 4.2A GeV/c along with the corresponding fits by the one-temperature

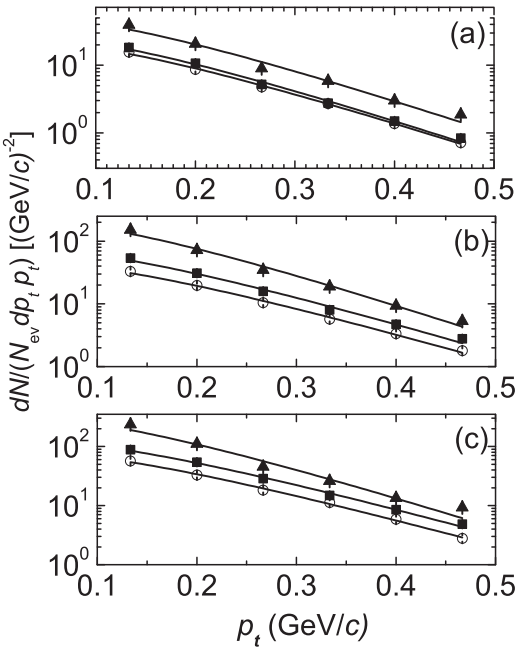

FIG. 4. Soft component of the experimental transverse momentum distributions of the negative pions in (a) peripheral, (b) semicentral, and (c) central $-^4$He+^{12}C (○), ^{12}C+^{12}C (■), and ^{12}C+^{181}Ta (▲) collisions at 4.2A GeV/c along with the corresponding fits (solid lines) by one-temperature Hagedorn function in the p_t range $0.1 - 0.5$ GeV/c.

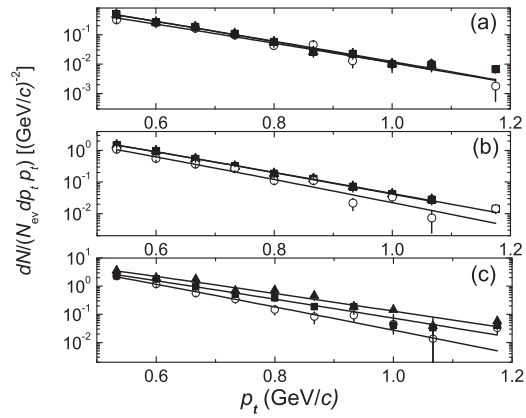

FIG. 5. Hard component of the experimental transverse momentum distributions of the negative pions in (a) peripheral, (b) semicentral, and (c) central $-^4$He+^{12}C (○), ^{12}C+^{12}C (■), and ^{12}C+^{181}Ta (▲) collisions at 4.2A GeV/c along with the corresponding fits (solid lines) by one-temperature Hagedorn function in the p_t range $0.5-1.2$ GeV/c.

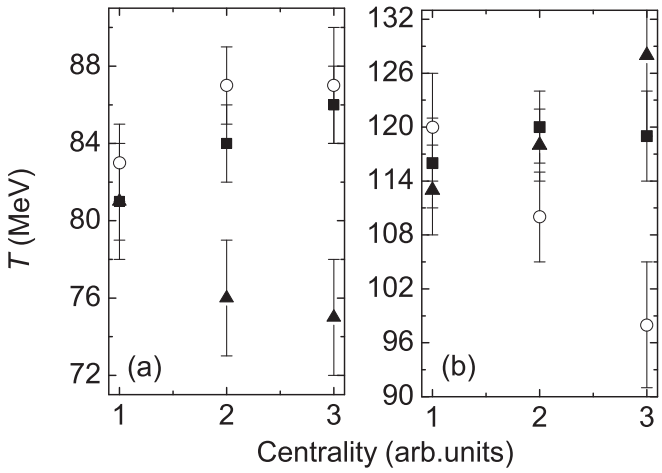

FIG. 6. Collision centrality dependence of the temperature of (a) soft and (b) hard components of the experimental transverse momentum distributions of the negative pions in ^{4}He+^{12}C (○), ^{12}C+^{12}C (■), and ^{12}C+^{181}Ta (▲) collisions at 4.2A GeV/c, extracted from fitting by one-temperature Hagedorn function in p_t range $0.1-0.5$ GeV/c and $0.5-1.2$ GeV/c, respectively. The numbers 1, 2, and 3 on the x axis correspond to the group of peripheral, semicentral, and central collision events, respectively.

Hagedorn function in the p_t range $0.5-1.2$ GeV/c. As seen from Figs. 4 and 5 and Table VI, both one-temperature Hagedorn and one-temperature Boltzmann functions describe quite satisfactorily the soft as well as hard components of the p_t distributions of π^- in three centrality groups in the studied collision systems.

Figure 6 demonstrates collision centrality dependencies of the temperatures of soft and hard components of the experimental p_t distributions of π^- in ^{4}He+^{12}C, ^{12}C+^{12}C, and ^{12}C+^{181}Ta collisions at 4.2A GeV/c, extracted from fitting by the one-temperature Hagedorn function in the p_t ranges $0.1-0.5$ GeV/c and $0.5-1.2$ GeV/c, respectively. As seen from Fig. 6, the temperatures of soft as well as hard components of p_t distributions of the negative pions in peripheral collisions are very close to each other for the collision systems under consideration. As observed from Fig. 6(a), on the whole, the gap between the temperatures of the soft p_t component in ^{4}He+^{12}C, ^{12}C+^{12}C, and ^{12}C+^{181}Ta collisions increases with an increase in collision centrality. The behavior of the centrality dependence of T of soft p_t component is, to a certain extent, close to each other for ^{4}He+^{12}C and ^{12}C+^{12}C collisions. For ^{12}C+^{12}C collisions, the T of soft p_t component increases with increasing centrality, whereas that for ^{4}He+^{12}C collisions first increases in going from peripheral to semicentral collisions, then remains almost constant in semicentral and central collisions. The centrality dependence of T of the soft p_t component for ^{12}C+^{181}Ta collisions demonstrates quite the opposite behavior: it decreases noticeably in going from peripheral to semicentral and central collisions. However, as can be noticed from Fig. 6(b), the temperature of the hard p_t component for ^{12}C+^{181}Ta collisions increases consistently with an increase in collision centrality, whereas that for ^{12}C+^{12}C collisions first increases in going from peripheral to semicentral collisions, then remains approximately constant in semicentral and central collisions. For ^{4}He+^{12}C collisions, the T of the hard p_t component decreases consistently with an increase in centrality. The observed differences between the behaviors of the centrality dependencies of T of both soft and hard p_t components of light and heavy collision systems can be analyzed in terms of the geometry and degree of overlap of colliding nuclei. The latter can be deduced from the numbers of participant projectile and target nucleons, and the corresponding number of binary (nucleon–nucleon) collisions.

The average numbers of participant nucleons from the projectile (A) and target (B) nuclei, and the corresponding average number of binary (nucleon–nucleon) collisions in the studied collision systems can be estimated by using the relations [59–61]

$$\langle \nu_A \rangle = \frac{A\sigma_{pB}^{\text{inel}}}{\sigma_{AB}^{\text{inel}}}, \tag{5}$$

$$\langle \nu_B \rangle = \frac{B\sigma_{pA}^{\text{inel}}}{\sigma_{AB}^{\text{inel}}}, \text{ and} \tag{6}$$

$$\langle \nu_{AB} \rangle = \frac{AB\sigma_{pp}^{\text{inel}}}{\sigma_{AB}^{\text{inel}}}, \tag{7}$$

respectively, where A and B are the total numbers of nucleons in the projectile and target nucleus, respectively, $\sigma_{pp}^{\text{inel}}$, $\sigma_{pA}^{\text{inel}}$, $\sigma_{pB}^{\text{inel}}$, and $\sigma_{AB}^{\text{inel}}$ are the inelastic cross sections of proton–proton, $p+A$, $p+B$, and $A+B$ collisions, taken from Refs. [62,63]. These relations were obtained [59,60] from the model of independent collisions of projectile nucleons with the target nucleons. This simple model accounts for only primary nucleon–nucleon collisions and disregards the cascading of the secondary nucleons. Table VII presents the inelastic cross sections and the average numbers of ν_A, ν_B, and ν_{AB}, calculated using the formulas in (5)–(7), along with the estimated average numbers of participant nucleons in the experiment in the studied collision systems at 4.2A GeV/c. The average numbers of participant nucleons in the studied nucleus–nucleus collisions at 4.2A GeV/c were estimated from the mean multiplicity per event of the participant protons in Table I, taking into account the

TABLE VII. The inelastic cross sections [62,63] and the average numbers of nucleon–nucleon collisions $\langle \nu_{AB} \rangle$, interacting projectile $\langle \nu_A \rangle$, and target $\langle \nu_B \rangle$ nucleons, calculated using a simple model of independent nucleon collisions [59,60], and the estimated average numbers of participant nucleons in nucleus–nucleus collisions at 4.2A GeV/c in the experiment.

Type	$p+p$	^{4}He+^{12}C	^{12}C+^{12}C	^{12}C+^{181}Ta
$\sigma^{inel}(A+B)$ (mb)	28 ± 1	450 ± 20	830 ± 50	3445 ± 140
$\langle \nu_A \rangle$	1	2.4 ± 0.2	3.8 ± 0.3	5.9 ± 0.3
$\langle \nu_B \rangle$	1	2.7 ± 0.2	3.8 ± 0.3	14.0 ± 1.0
$\langle \nu_{AB} \rangle$	1	3.0 ± 0.2	4.9 ± 0.3	18.0 ± 1.0
$\langle \nu_A \rangle + \langle \nu_B \rangle$	2	5.1 ± 0.3	7.6 ± 0.4	20.0 ± 1.0
$\langle n_{\text{part..nucl..}} \rangle^{\text{exper}}$	2	5.66 ± 0.04	8.70 ± 0.04	32.5 ± 0.5

corresponding ratio of neutrons and protons in each collision system. As noticed from Table VII, ^{12}C+^{181}Ta collisions are characterized by significantly larger average numbers of binary (nucleon–nucleon) collisions, participant projectile and target nucleons, as compared to those in ^{4}He+^{12}C and ^{12}C+^{12}C collisions. As seen from a comparison of the calculated and experimental average numbers of participant nucleons in Table VII, the contribution of the secondary cascading processes, neglected in the model, increases with an increase in size of a collision system. From a comparison of the numbers of participant nucleons in this simple model and the experiment in Table VII, we estimated that the secondary cascading processes contribute approximately 10%, 13%, and 38% to the formation of participant nucleons in ^{4}He+^{12}C, ^{12}C+^{12}C, and ^{12}C+^{181}Ta collisions, respectively.

As deduced from analysis of relativistic heavy ion collisions [64], the contribution of soft processes scales with the number of participant nucleons and that of semi(hard) scattering processes scales with the number of binary (nucleon–nucleon) collisions. Hence, it is expected that the contribution of both soft and hard processes should be significantly larger in the case of the heavy ^{12}C+^{181}Ta collision system as compared to the light ^{4}He+^{12}C and ^{12}C+^{12}C systems. This supports our observation that the temperature of hard p_t component for ^{12}C+^{181}Ta collisions increases with an increase in collision centrality [which corresponds to an increase of binary collisions, resulting in a significant increase of probability of (semi)hard nucleon–nucleon scatterings]. The pions in this hard p_t range originate mostly from an early fast stage of nuclear collisions. In terms of collective flow effects, these pions are thought to come from the early stage of the collision (before chemical freeze-out) from the initial fast component of the collective flow, built up by the high pressure in a core of the collision zone [64]. According to the QGSM calculations for nucleus–nucleus collisions at $4.2A$ GeV/c [20,21], the major fraction of pions (≈70% on the average) in the soft p_t range originates at a later stage from decays of Δ resonances and vector mesons, such as ρ, ω, and η, when the collision system cools down noticeably. In the soft p_t range ($p_t < 0.5$ GeV/c), according to QGSM, a fraction of pions, coming from Δ and vector meson decays, increases with increasing the collision system-size in nucleus–nucleus collisions at $4.2A$ GeV/c [20,21]. On the other hand, the hard p_t range ($p_t > 0.5$ GeV/c), in this model, is dominated (≈55% on the average) by pions produced directly in nucleon–nucleon collisions as $NN \rightarrow NN\pi$ [20,21].

The observed centrality dependence of T in the soft p_t range in the studied reactions could be interpreted in terms of fireball creation, expansion, and its chemical and final kinetic freeze-out, as was discussed for Au + Au collisions at relativistic heavy ion collision (RHIC) energies in Ref. [64]. The main difference is that, at our collision energy ($\sqrt{s_{NN}} =$ 3.14 GeV), the fireball is expected to be compressed and dense nuclear (nucleon) matter, whereas at RHIC energies the fireball can be associated with the quark gluon plasma, a state of deconfined quarks and gluons. The threshold c.m. collision energy $\sqrt{s_{NN}} \approx 5$ GeV was estimated for reaching the deconfinement threshold energy density from lattice QCD calculations [65]. Therefore, it is expected that a significant fraction of the collision system should undergo transition to the QGP in central heavy ion collisions at RHIC energies, much larger than $\sqrt{s_{NN}} = 5$ GeV. After the expansion and chemical freeze-out of a compressed nuclear matter, or a nuclear (nucleon) fireball, created in central ^{12}C+^{181}Ta collisions, the produced pions undergo multiple elastic scatterings with the surrounding nucleons of a heavy target medium and, hence, their temperature drops noticeably at the final kinetic freeze-out.

The observed centrality dependence of T in the soft p_t range in ^{12}C+^{181}Ta collisions could be explained qualitatively in a simpler way. As $A_p \ll A_t$ in ^{12}C+^{181}Ta collisions, the energy of impinging projectile nucleons has to be distributed among more and more nucleons of heavy ^{181}Ta target as the collision centrality increases. In case of central ^{12}C+^{181}Ta collisions, each of the incoming projectile nucleons invokes at least several nucleon–nucleon collisions (interactions) with heavy target nucleons, which results in a significantly higher multiplicity of pions produced on tantalum nuclei in central ^{12}C+^{181}Ta collisions as compared to peripheral ^{12}C+^{181}Ta collisions, where significantly lesser pions are produced, mostly in the first single collisions (interactions) of projectile nucleons with target nucleons [35]. Indeed, as observed in Fig. 1(b), the significantly larger number of π^- mesons is produced in around the heavy target fragmentation region as compared to the light projectile fragmentation region. Hence, in the case of central ^{12}C+^{181}Ta collisions, the collision energy is distributed among a significantly larger number of pions compared to peripheral ^{12}C+^{181}Ta collisions, which results in lower mean kinetic energies of π^- in central ^{12}C+^{181}Ta collisions as compared to the peripheral ones [35]. Hence, the T of the soft p_t component decreases with increasing centrality of ^{12}C+^{181}Ta collisions.

In contrast to ^{12}C+^{181}Ta collisions, quite the opposite trend in behavior of the centrality dependence of T of the soft p_t component in ^{4}He+^{12}C and ^{12}C+^{12}C collisions, observed in Fig. 6(a), can be interpreted as due to the much smaller system size and, hence, much lesser probability of multiple rescatterings of pions after the chemical freeze-out stage. The small difference in behavior of the centrality dependence of T of the soft p_t component in ^{4}He+^{12}C and ^{12}C+^{12}C collisions in Fig. 6(a) can be explained by the difference in the geometry of these collision systems. As $A_p < A_t$ in ^{4}He+^{12}C collisions, we expect a complete overlap of these colliding nuclei already in semicentral collisions. Therefore, after the initial growth of T of the soft p_t component in ^{4}He+^{12}C collisions in going from peripheral to semicentral collisions, practically no more appreciable energy can be transferred from target to projectile nucleons in the range from semicentral to central collisions. Hence, the temperature of the soft p_t component remains constant for semicentral and central ^{4}He+^{12}C collisions. As $A_p = A_t$ in ^{12}C+^{12}C collisions, we expect the consistent growth of the degree of overlap of these colliding nuclei with an increase in centrality in going from peripheral to central collisions. Therefore, the energy transferred from projectile to target nucleons and T of the soft p_t component increases with increasing centrality of ^{12}C+^{12}C collisions. In the above, an increase of the energy, transferred from projectile to target nucleons with increasing centrality can also be thought as an

increase in the compressional energy of compressed nuclear matter [or nuclear (nucleon) fireball] in semicentral and central ^{12}C+^{12}C collisions.

In ^{4}He+^{12}C and ^{12}C+^{12}C collision systems, both the projectile and target nuclei have equal numbers of protons and neutrons. On the other hand, in the ^{12}C+^{181}Ta collision system, the number of neutrons is almost 1.5 times greater than that of protons in the heavy ^{181}Ta target nucleus. Hence, the fraction as well as the number of interactions (collisions) of projectile nucleons with target neutrons is significantly greater in ^{12}C+^{181}Ta collisions as compared to ^{4}He+^{12}C and ^{12}C+^{12}C collisions. This increases significantly the fraction of π^- coming from the decay of neutral baryon resonances in the case of ^{12}C+^{181}Ta collisions as compared to those in ^{4}He+^{12}C and ^{12}C+^{12}C collisions. Indeed, it was estimated experimentally that about half of the negative pions come from the decay of Δ^0 resonances in ^{12}C+^{12}C [8] and ^{4}He+^{12}C [4] collisions at 4.2A GeV/c, whereas the corresponding estimated fraction of π^- from Δ^0 decay was around 2/3 in ^{12}C+^{181}Ta collisions [11] at 4.2A GeV/c. As shown in Table VII, the average number of binary collisions in ^{12}C+^{181}Ta collisions is at least around five to six times greater than that in ^{4}He+^{12}C and ^{12}C+^{12}C collisions. In addition, the contribution of the secondary cascading processes to the formation of participant nucleons was significantly larger in ^{12}C+^{181}Ta collisions (38%), as compared to ^{4}He+^{12}C (10%) and ^{12}C+^{12}C (13%) collisions. Hence, it is expected that the fraction of the negative pions coming from the decay of Δ resonances will increase with increasing centrality of ^{12}C+^{181}Ta collisions.

As already mentioned, the consistent increase of T of the hard p_t component in ^{12}C+^{181}Ta collisions, observed in Fig. 6(b), can be explained either by the early fast component of the collective flow resulting from the high pressure, built up in a core of the collision zone, in central collisions, or by an increase of the probability of semi(hard) scatterings with an increase in collision centrality, which scales with the number of binary collisions. In the case of ^{12}C+^{12}C collisions, the temperature of the hard p_t component first increases in going from peripheral to semicentral collisions, then it remains almost constant for semicentral and central collisions. This is likely due to the relative smallness of both the identical projectile and target nucleus. Hence, we do not expect any appreciable increase in the pressure, built up in a core of the collision zone, in going from semicentral to central ^{12}C+^{12}C collisions. For the even smaller ^{4}He+^{12}C collision system, the probability of the production of a dense nuclear (nucleon) fireball in semicentral and central collisions is expected to be extremely low, if not zero. Therefore, the decrease of T of the hard p_t component with increasing centrality of ^{4}He+^{12}C collisions can be explained in terms of simple semi(hard) nucleon–nucleon collisions. In the case of peripheral ^{4}He+^{12}C collisions, quite energetic pions produced in semi(hard) nucleon–nucleon collisions (from small overlap zone at periphery of colliding nuclei) will most probably escape the collision zone without further rescattering. With an increase in collision centrality, the path to be traversed through the target ^{12}C nucleus, along the direction of the impinging projectile nucleon, increases from zero to $2R(^{12}\mathrm{C})$ [where $R(^{12}\mathrm{C})$ is the radius of the ^{12}C nucleus] in going from most peripheral to most central ^{4}He+^{12}C collisions. Hence, the rescattering probability of a pion, produced in a semi(hard) nucleon–nucleon collision, on surrounding target nucleons increases with increasing centrality of ^{4}He+^{12}C collisions. This can explain qualitatively the decrease of T of the hard p_t component with increasing centrality of ^{4}He+^{12}C collisions, observed in Fig. 6(b).

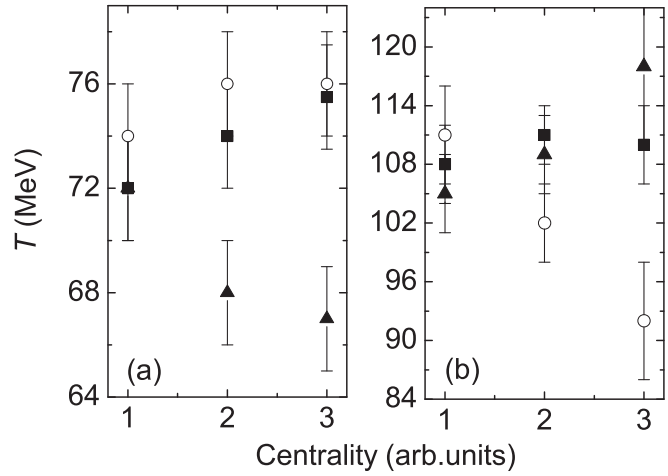

FIG. 7. The same as in Fig. 6, but extracted from fitting by one-temperature Boltzmann function.

As seen from Fig. 7, the temperatures extracted using the one-temperature Boltzmann function reproduces completely the behavior of centrality dependences of T of both the soft and hard p_t components of π^-, observed in Fig. 6.

Figure 8 presents collision system-size dependencies of the temperatures of soft and hard components of the experimental

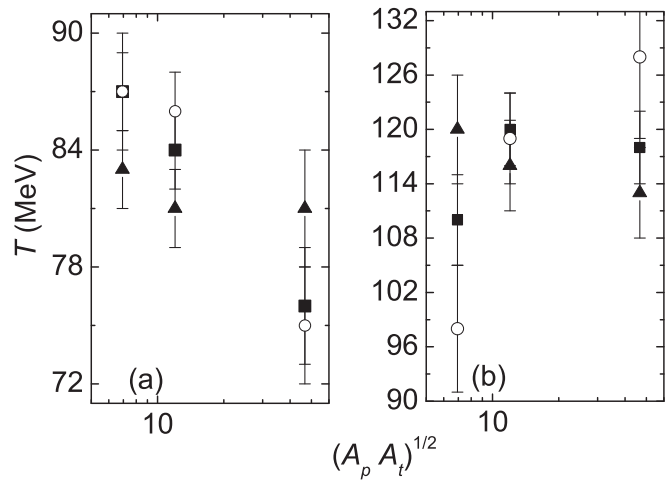

FIG. 8. Collision system-size dependence of the temperature of (a) soft and (b) hard components of the experimental transverse momentum distributions of the negative pions in peripheral (▲), semicentral (■), and central (○) nucleus–nucleus collisions at 4.2A GeV/c, extracted from fitting by one-temperature Hagedorn function in the p_t range $0.1 - 0.5$ GeV/c and $0.5 - 1.2$ GeV/c, respectively.

p_t distributions of π^- in peripheral, semicentral, and central nucleus–nucleus collisions at $4.2A$ GeV/c, extracted from fitting by the one-temperature Hagedorn function in the p_t ranges $0.1 - 0.5$ GeV/c and $0.5 - 1.2$ GeV/c, respectively. As observed from Fig. 8(a), the temperatures of the soft p_t component for semicentral and central collisions decreases consistently with an increase in system size $[(A_pA_t)^{1/2}]$, or, in other words, with an increase in the number of participant nucleons in collision systems. On the other hand, the temperature of the soft p_t component for peripheral collisions does not change appreciably with an increase in collision system-size. The decrease of T in semicentral and central collisions in going from ^{4}He+^{12}C to ^{12}C+^{12}C and ^{12}C+^{181}Ta collisions can be interpreted in terms of the nuclear (nucleon) fireball creation as well as by an increase of the fraction of the "cold" negative pions, coming from the decay of delta resonances. As already mentioned, with an increase in system size, the pions undergo more and more elastic rescaterrings on the nucleons of the surrounding medium until they reach the final kinetic freeze-out stage, where the system is cooled down significantly. Evidently, no nuclear (nucleon) fireball is expected to be produced in peripheral nucleus–nucleus collisions. Peripheral interactions of nuclei proceed at significantly lower momentum–energy transfers with a markedly lesser number of pions (as well as with a considerably smaller fraction of π^- from resonance decays) as compared to semicentral and central collisions. Due to the short range of strong interactions, only relatively small fractions (at the periphery of nuclei) of colliding nuclei can be involved in a strong interaction in peripheral collisions. Hence, the size of the colliding nuclei does not play a noticeable role in peripheral collisions and, therefore, the temperature of the soft p_t component does not vary appreciably with an increase in $(A_pA_t)^{1/2}$ in these interactions.

Here it is worth mentioning the results of Ref. [46], where the light front analysis of the negative pions in central He + (Li, C), C + Ne, C + Cu, and O + Pb collisions at $4.5A$ GeV/c was performed. The phase space of the secondary pions was divided into two parts, in one of which the thermal equilibrium assumption seemed to be in good agreement with the data. The thermal equilibrium region corresponded to a lower p_t range ($p_t < 0.4$ GeV/c) [46]. The corresponding temperatures were extracted from fitting the data by the Boltzmann distribution function. The dependence of the obtained T on $(A_pA_t)^{1/2}$ was studied. The temperature decreased consistently with an increase in $(A_pA_t)^{1/2}$ [46]. This is in agreement with a decrease of T of the soft p_t component of π^- with increasing of the system size in semicentral and central nucleus–nucleus collisions at $4.2A$ GeV/c, obtained in the present work. The temperatures of the soft p_t component extracted in the present analysis are comparable to the corresponding temperatures obtained by the authors of Ref. [46]. However, no physical interpretation for a decrease of T with an increase in $(A_pA_t)^{1/2}$ was given in Ref. [46].

As observed from Fig. 8(b), the T of the hard p_t component in central collisions increases consistently with an increase in system size. This can be understood in terms of semi(hard) nucleon–nucleon collisions. Such an increase of the temperature of the hard p_t component in central collisions with an increase in the system size can be explained as follows. This is because, as was already mentioned, the probability of semi(hard) nucleon–nucleon collisions increases significantly as the number of binary collisions increases quite prominently in going from central ^{4}He+^{12}C to central ^{12}C+^{12}C collisions, and further to central ^{12}C+^{181}Ta collisions. Indeed, since $A(^{181}\text{Ta}) \gg A(^{12}\text{C}) > A(^4\text{He})$, the probability of semi(hard) scattering of the projectile nucleon with the target nucleon will be greater in the case of central ^{12}C+^{181}Ta collisions as compared to central ^{12}C+^{12}C and ^{4}He+^{12}C collisions. Hence, the T of the hard p_t component in central collisions increases with an increase in $(A_pA_t)^{1/2}$. This can also be explained by an increase in pressure, built up in a core of the collision zone (and, hence, by an increase of T of "hot" pions coming out of this core at the initial collision stage), with an increase in $(A_pA_t)^{1/2}$ in central nucleus–nucleus collisions. Indeed, since the ^{181}Ta target is much heavier than the light ^{12}C target, the extent of the compressibility of a nuclear matter, and hence the pressure attained in central nucleus–nucleus collisions, is expected to be larger in the case of central ^{12}C+^{181}Ta collisions as compared to central ^{12}C+^{12}C and ^{4}He+^{12}C collisions.

As seen from Fig. 8(b), the T of the hard p_t component shows only a weak decrease with an increase in $(A_pA_t)^{1/2}$ in peripheral nucleus–nucleus collisions at $4.2A$ GeV/c. Such a weak dependence of T on $(A_pA_t)^{1/2}$, as already discussed, is likely due to a small degree of overlap, at the periphery of colliding nuclei, in peripheral interactions. Though an overlap of the colliding nuclei is relatively small in peripheral collisions, the probability of further rescattering of pions, produced in semi(hard) nucleon–nucleon collisions, on the target nucleons is greater in ^{12}C+^{181}Ta as compared to ^{12}C+^{12}C and ^{4}He+^{12}C collisions due to still some differences in the sizes of the overlap regions in the peripheral interactions since $A(^{181}\text{Ta}) \gg A(^{12}\text{C}) > A(^4\text{He})$. In semicentral collisions, as observed from Fig. 8(b), the T of the hard p_t component is larger in heavier ^{12}C+^{12}C and ^{12}C+^{181}Ta collision systems as compared to the lighter ^{4}He+^{12}C system, which is likely due to the larger size of the overlap region in the heavier systems as compared to the lighter one.

Figure 9 shows that the temperatures extracted using the one-temperature Boltzmann function reproduce completely the behavior of the system-size dependencies of T of both the soft and hard p_t components of π^-, observed in Fig. 8.

Finally, it is of importance to discuss some quantitative results on values of T, obtained for pions in other JINR, GSI, and SPS experiments to link the quantitative findings of the present work with those obtained at lower, intermediate, and higher energies. In Ref. [66] the temperatures of the negative pions in central Mg + Mg collisions at $4.3A$ GeV/c (GIBS setup of JINR) were estimated from inclusive kinetic energy and transverse momentum spectra of π^- mesons using two different selection criteria: in the rapidity interval 0.5–2.1 (corresponding to π^- pionization region) and at c.m.s. angles (90 ± 10) degrees. The pion spectra were fitted by a sum of two exponentials with two temperatures, $T_1 = 55 \pm 1$ MeV and $T_2 = 113 \pm 2$ MeV. The relative yield of the second exponential term having a temperature T_2 was about 22%. These

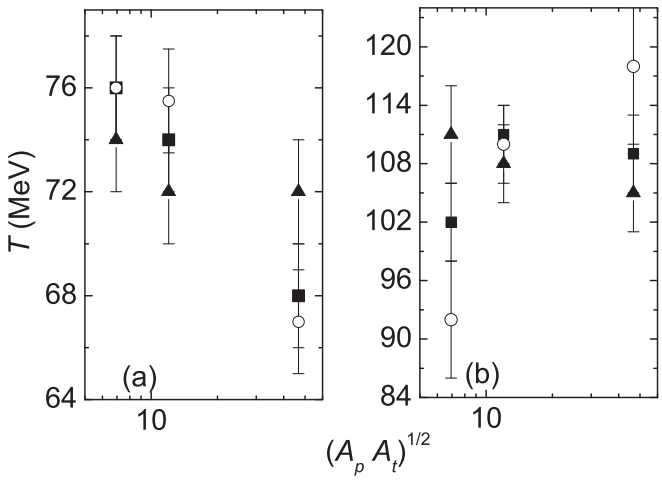

FIG. 9. The same as in Fig. 8, but extracted from fitting by one-temperature Boltzmann function.

values of T_1 and T_2 are comparable to the corresponding T_1 and T_2 values extracted in central nucleus–nucleus collisions at $4.2A$ GeV/c in the present analysis (see Table V). The light front analysis of the negative pions in central He(Li, C), C + Ne, C + Cu and O + Pb collisions at $4.5A$ GeV/c was made in Ref. [46]. The phase space of secondary pions was divided into two parts, into one of which the thermal equilibrium seemed to be in a good agreement with the data. The thermal equilibrium region corresponded to the lower p_t range ($p_t < 0.4$ GeV/c) [46]. The extracted temperatures proved to be 81 ± 2, 79 ± 3, 72 ± 2, and 55 ± 3 MeV in central He(Li, C), C + Ne, C + Cu, and O + Pb collisions at $4.5A$ GeV/c, respectively [46]. The temperature obtained in central He(Li, C) collisions at $4.5A$ GeV/c is compatible with the temperature of the soft p_t component of π^- mesons in central ^{4}He+^{12}C collisions at $4.2A$ GeV/c, extracted in the present analysis (see Table VI). Also the temperatures extracted in central C + Ne and C + Cu collisions at $4.5A$ GeV/c [46] are comparable to the corresponding temperatures of the soft p_t component of π^- mesons in central ^{12}C+^{12}C and ^{12}C+^{181}Ta collisions, respectively, extracted in the present work (see Table VI).

The values of T for pions were extracted also in GSI experiments (FOPI, FRS, KAON, and TAPS Collaborations) [67–72]. It was deduced that the spectra of π^- mesons in central Ni + Ni collisions at incident (kinetic) energies $E_{\rm kin} = 1.06A$ GeV, $1.45A$ GeV, and $1.93A$ GeV (FOPI Collaboration [67]) required the sum of two exponentials with independent yields and inverse slope parameters T_l and T_h describing mainly the low and high momentum parts of the spectrum, respectively. $T_l = 55 \pm 3$ MeV and $T_h = 93 \pm 5$ MeV, and $T_l = 56 \pm 3$ MeV and $T_h = 100 \pm 5$ MeV, and $T_l = 61 \pm 3$ MeV and $T_h = 115 \pm 6$ MeV were extracted at $E_{\rm kin} = 1.06A$ GeV, $1.45A$ GeV, and $1.93A$ GeV, respectively. In Ne + NaF collisions (FRS Collaboration) the T for π^- mesons ranged from 78 ± 2 MeV to 96 ± 3 MeV for projectile energies from $1.34A$ to $1.94A$ GeV. The KAON Collaboration extracted the value of T for π^+ mesons to be 71 ± 3 MeV and 95 ± 3 MeV for projectile energies $1A$ GeV and $1.8A$ GeV, respectively. The TAPS Collaboration obtained a T value for π^0 mesons to be 83 ± 3 MeV in C +C collisions at $E_{\rm kin} = 2A$ GeV and $T = 70 \pm 1$ MeV in Ar + Ca collisions at $E_{\rm kin} = 1.5A$ GeV. Significantly larger inverse slope parameters (apparent temperatures) T ranging from around 140 to 160 MeV were extracted in SPS experiments by the NA44 Collaboration [55,73] for charged pions from fitting their transverse mass spectra with the simple Boltzmann distribution in central Pb + Pb and S + S collisions at $158A$ GeV/c and $200A$ GeV/c, respectively. On the whole, the temperatures extracted from pion spectra in central nucleus–nucleus collisions (GSI, JINR, SPS experiments) depended on the collision energy and sizes (geometry) of the colliding nuclei.

V. SUMMARY AND CONCLUSIONS

We analyzed the collision centrality as well as the system-size dependencies of the temperatures of the soft ($p_t = 0.1-0.5$ GeV/c) and hard ($p_t = 0.5 - 1.2$GeV/c) parts of the experimental transverse momentum distributions of the negative pions in ^{4}He+^{12}C, ^{12}C+^{12}C, and ^{12}C+^{181}Ta collisions at $4.2A$ GeV/c ($\sqrt{s_{NN}} = 3.14$ GeV). For the studied collision systems and selected collision centralities, the temperatures were extracted from fitting separately the soft and hard components of p_t distributions of π^- mesons by one-temperature Hagedorn as well as one-temperature Boltzmann functions. The temperatures extracted using the one-temperature Boltzmann function reproduced completely the observed collision centrality and system-size dependencies of the temperatures of both the soft and hard p_t components, obtained from fitting by the one-temperature Hagedorn function.

The extracted temperatures of both the soft and hard components of p_t distributions of π^- depended on the geometry (size) and degree of overlap of colliding nuclei in peripheral, semicentral, and central ^{4}He+^{12}C, ^{12}C+^{12}C, and ^{12}C+^{181}Ta collisions at $\sqrt{s_{NN}} = 3.14$ GeV. The differences between the extracted temperatures in the studied collision systems increased with increasing the degree of overlap of colliding nuclei (i.e., with an increase in collision centrality) and the corresponding increase in the numbers of participant nucleons and binary collisions.

The behavior of centrality dependence and values of T of the soft p_t component of π^- proved to be close to each other in ^{4}He+^{12}C and ^{12}C+^{12}C collision systems. The temperature of the soft p_t component of the negative pions in ^{12}C+^{12}C (^{12}C+^{181}Ta) collisions increases (decreases) with the increasing of the collision centrality. The temperature of the hard p_t component of π^- in ^{12}C+^{181}Ta (^{4}He+^{12}C) collisions increases (decreases) consistently with an increase in collision centrality. The physical interpretations of the observed centrality dependencies of T in the studied collision systems are given.

The temperature of the soft p_t component for π^- decreases consistently with an increase in system size $[(A_pA_t)^{1/2}]$ in the semicentral and central nucleus–nucleus collisions at $4.2A$ GeV/c. This agrees with the decrease of T of π^- with increasing $(A_pA_t)^{1/2}$ obtained in Ref. [46] using the light front analysis of the negative pions in central He + (Li, C), C + Ne, C + Cu, and O + Pb collisions at 4.5 A GeV/c. The

decrease of T of the soft p_t component in semicentral and central collisions in going from ^{4}He+^{12}C to ^{12}C+^{12}C and ^{12}C+^{181}Ta collisions can be interpreted in terms of the nuclear (nucleon) fireball creation, expansion, and its chemical and final kinetic freeze-out. With an increase in system size, the pions have to undergo more and more rescatterings on nucleons of the surrounding medium until they reach the final kinetic freeze-out stage, where the system is cooled down appreciably.

Such a decrease of T of the soft p_t component of π^- with an increase in $(A_pA_t)^{1/2}$ can also be interpreted qualitatively in a simpler way. In contrast to semicentral and central ^{4}He+^{12}C and ^{12}C+^{12}C collisions, in semicentral and central ^{12}C+^{181}Ta collisions, the energy of the impinging (projectile) nucleons has to be distributed among significantly larger numbers of participant (target) nucleons and the produced pions. Hence, this results in a lesser average kinetic energy of π^- in the soft p_t range in ^{12}C+^{181}Ta collisions as compared to those in ^{4}He+^{12}C and ^{12}C+^{12}C collisions.

In central collisions, the temperature of the hard p_t component of π^- increases consistently with an increase in system size. This hard p_t component can be explained as mainly due to pions produced in semi(hard) nucleon–nucleon collisions. Such an increase of T of the hard p_t component in central collisions with increasing of the system size is in line with the following: the probability of semi(hard) nucleon–nucleon collisions increases as the number of binary collisions increases quite prominently in going from central ^{4}He+^{12}C to central ^{12}C+^{12}C collisions, and further to central ^{12}C+^{181}Ta collisions. Indeed, since $A(^{181}\text{Ta}) \gg A(^{12}\text{C}) > A(^4\text{He})$, the probability of semi(hard) scattering of the projectile nucleon with the target nucleon will be greater in the case of central ^{12}C+^{181}Ta collisions as compared to central ^{12}C+^{12}C and ^{4}He+^{12}C collisions. The increase of T of the hard p_t component in central collisions can also be interpreted by an increase in pressure, built up in a core of the collision zone (and, hence, by an increase of T of "hot" pions emitted from this core at the initial collision stage), with an increase in $(A_pA_t)^{1/2}$ in central nucleus–nucleus collisions.

The quantitative results on T for the negative pions in nucleus–nucleus collisions at 4.2A GeV/c, extracted in the present work, were compared and linked to those obtained in lower, intermediate, and higher energies in other JINR, GSI, and SPS experiments.

ACKNOWLEDGMENTS

We are grateful to the staff of the Laboratory of High Energies of JINR (Dubna, Russia) and of the Laboratory of Multiple Processes of Physical-Technical Institute of Uzbek Academy of Sciences (Tashkent, Uzbekistan) who participated in the processing of stereophotographs from 2-m propane bubble chamber of JINR and increasing significantly the corresponding statistics of nucleus–nucleus collisions at 4.2A GeV/c. We are thankful to R. Bekmirzaev and N. Amelin (JINR) for providing us the data of simulated QGSM collision events. A.I. and M.Q.H. acknowledge partial support from Higher Education Commission of Pakistan (HEC) Research Project No. 1925.

[1] P. Braun-Munzinger and J. Stachel, Pion production in heavy ion collisions, Ann. Rev. Nucl. Part. Sci. **37**, 97 (1987).
[2] R. Stock *et al.*, Compression effects in relativistic nucleus-nucleus collisions, Phys. Rev. Lett. **49**, 1236 (1982).
[3] Kh. K. Olimov, M. Q. Haseeb, and I. Khan, Comparison of characteristics of $\Delta^0(1232)$ produced in p ^{12}C and d ^{12}C collisions at 4.2A GeV/c, Phys. At. Nucl. **75**, 479 (2012).
[4] Kh. K. Olimov *et al.*, Production of Δ^0 and Δ^{++} resonances in collisions of ^{4}He nuclei with carbon nuclei at 4.2 GeV/c per nucleon, Phys. Rev. C **75**, 067901 (2007).
[5] Kh. K. Olimov, M. Q. Haseeb, I. Khan, A. K. Olimov, and V. V. Glagolev, Δ^0 (1232) production in d + ^{12}C collisions at 4.2 A GeV/c, Phys. Rev. C **85**, 014907 (2012).
[6] Kh. K. Olimov and M. Q. Haseeb, Production of $\Delta^0(1232)$-resonances in p + ^{12}C collisions at a momentum of 4.2 GeV/c, Eur. Phys. J. A **47**, 79 (2011).
[7] Kh. K. Olimov, M. Q. Haseeb, A. K. Olimov, and I. Khan, Analysis of $\Delta^0(1232)$ production in collisions of protons with carbon nuclei at 4.2 GeV/c, Centr. Eur. J. Phys. **9**, 1393 (2011).
[8] D. Krpic, G. Skoro, I. Picuric, S. Backovic, and S. Drndarevic, Baryon resonances in carbon–carbon collisions at 4.2 GeV/c per nucleon, Phys. Rev. C **65**, 034909 (2002).
[9] Kh. K. Olimov, Production of baryon resonances in π^- + ^{12}C interactions at 40 GeV/c, Phys. Rev. C **76**, 055202 (2007).
[10] Kh. K. Olimov, S. L. Lutpullaev, B. S. Yuldashev, Y. H. Huseynaliyev, and A. K. Olimov, Production of $\Delta(1232)$ resonances on oxygen nuclei in ^{16}O+p collisions at a momentum of 3.25 GeV/c per nucleon, Eur. Phys. J. A **44**, 43 (2010).
[11] Kh. K. Olimov, Production of delta isobars on tantalum nuclei in CTa-collisions at a projectile momentum of 4.2 GeV/c per nucleon, Phys. At. Nucl. **73**, 433 (2010).
[12] B.-A. Li and C. M. Ko, Formation of superdense hadronic matter in high energy heavy-ion collisions, Phys. Rev. C **52**, 2037 (1995).
[13] W. Ehehalt, W. Cassing, A. Engel, U. Mosel, and Gy. Wolf, Effects of pion and delta selfenergies in nucleus–nucleus reactions, Phys. Lett. B **298**, 31 (1993).
[14] M. Eskef *et al.* (FOPI Collaboration), Identification of baryon resonances in central heavy-ion collisions at energies between 1 and 2 A GeV, Eur. Phys. J. A **3**, 335 (1998).
[15] J. Barrette *et al.* (E814 Collaboration), Measurement of pion enhancement at low transverse momentum and of the Δ resonance abundance in Si-nucleus collisions at AGS energy, Phys. Lett. B **351**, 93 (1995).
[16] G. E. Brown, J. Stachel, and G. M. Welke, Pions from resonance decay in Brookhaven relativistic heavy-ion collisions, Phys. Lett. B **253**, 19 (1991).
[17] B.-A. Li and W. Bauer, Pion spectra in a hadronic transport model for relativistic heavy ion collisions, Phys. Rev. C **44**, 450 (1991).
[18] P. K. Netrakanti and B. Mohanty, The width of rapidity distribution in heavy ion collisions, Phys. Rev. C **71**, 047901 (2005).
[19] Lj. Simic *et al.*, Centrality dependence of pion and proton spectra in C+C and C+Ta interactions at 4.2 GeV/c per nucleon, Phys. Rev. C **52**, 356 (1995).

[20] R. N. Bekmirzaev, E. N. Kladnitskaya, and S. A. Sharipova, Rapidity distributions of π^- mesons in (p, d, α, C) C interactions at 4.2 GeV/c per nucleon, Phys. Atom. Nucl. **58**, 58 (1995).

[21] R. N. Bekmirzaev, E. N. Kladnitskaya, M. M. Muminov, and S. A. Sharipova, Rapidity distributions of π^- in (d, α, C) Ta collisions at 4.2 GeV/c per nucleon, Phys. Atom. Nucl. **58**, 1721 (1995).

[22] L. Chkhaidze, T. Djobava, L. Kharkhelauri, and M. Mosidze, The comparison of characteristics of π^- mesons produced in central Mg+Mg interactions with the quark gluon string model predictions, Eur. Phys. J. A **1**, 299 (1998).

[23] Kh. K. Olimov, A. Iqbal, V. V. Glagolev, and M. Q. Haseeb, Analysis of rapidity spectra of negative pions in $d + {}^{12}$C, ${}^{12}\mathrm{C} + {}^{12}\mathrm{C}$, and ${}^{12}\mathrm{C} + {}^{181}$Ta collisions at 4.2 GeV/c per nucleon, Phys. Rev. C **88**, 064903 (2013).

[24] J. L. Klay *et al.* (E895 Collaboration), Longitudinal Flow of Protons from $(2-8)A$ GeV Central Au + Au Collisions, Phys. Rev. Lett. **88**, 102301 (2002).

[25] J. Aichelin and K. Werner, A novel approach to rescattering in ultrarelativistic heavy ion collisions, Phys. Lett. B **300**, 158 (1993).

[26] B. Mohanty and J. Alam, Velocity of sound in relativistic heavy-ion collisions, Phys. Rev. C **68**, 064903 (2003).

[27] S. Backovic *et al.*, Temperature of negative pions in inelastic (d, α, C) + (C, Ta) collisions at 4.2A GeV/c, Phys. Rev. C **46**, 1501 (1992).

[28] R. Brockmann *et al.*, "Pion and Proton" Temperatures in Relativistic Heavy-Ion Reactions, Phys. Rev. Lett. **53**, 2012 (1984).

[29] L. Chkhaidze *et al.*, The temperatures of protons and π^- mesons in central nucleus-nucleus interactions at a momentum of 4.5 GeV/c per incident nucleon, Z. Phys. C **54**, 179 (1992).

[30] Kh. K. Olimov *et al.*, Centrality dependences of soft and hard components of p_t distributions of negative pions in ${}^4\mathrm{He} + {}^{12}\mathrm{C}$ collisions at 4.2A GeV/c, Int. J. Mod. Phys. E **24**, 1550036 (2015).

[31] L. Chkhaidze, T. Djobava, and L. Kharkhelauri, Temperatures of Λ hyperons, K^0 and π^- mesons produced in C-C and Mg-Mg collisions at 4.2–4.3 A GeV/c, Bull. Georg. Natl. Acad. Sci. **4**, 41 (2010).

[32] L. Chkhaidze *et al.*, Anisotropic collective flow of Λ-hyperons produced in C+C collisions at 4.2A GeV/c, Nucl. Phys. A **831**, 22 (2009).

[33] Kh. K. Olimov and M. Q. Haseeb, On spectral temperatures of negative pions produced in $d\,{}^{12}$C, ^{4}He ^{12}C, and ^{12}C ^{12}C collisions at 4.2 A GeV/c, Phys. At. Nucl. **76**, 595 (2013).

[34] A. Iqbal *et al.*, On centrality and rapidity dependences of transverse momentum spectra of negative pions in ${}^{12}\mathrm{C} + {}^{12}\mathrm{C}$ collisions at 4.2 GeV/c per nucleon, Int. J. Mod. Phys. E **23**, 1450047 (2014).

[35] Kh. K. Olimov *et al.*, On transverse momentum spectra of negative pions in ${}^{12}\mathrm{C} + {}^{181}$Ta collisions at 4.2$A$ GeV/c per nucleon, Int. J. Mod. Phys. E **23**, 1450084 (2014).

[36] Kh. K. Olimov, M. Q. Haseeb, and S. A. Hadi, Rapidity and angular dependences of spectral temperatures of negative pions produced in ${}^{12}\mathrm{C} + {}^{12}\mathrm{C}$ collisions at 4.2 A GeV/c, Int. J. Mod. Phys. E **22**, 1350020 (2013).

[37] R. Hagedorn and J. Rafelski, Hot hadronic matter and nuclear collisions, Phys. Lett. B **97**, 136 (1980).

[38] S. Backovic *et al.*, The Boltzmann temperature of negative pions in inelastic (d, α, C) + (C, Ta) collisions at 4.2A GeV/c, JINR Rapid Communications No. 2 [53]-92, 58 (Dubna, 1992).

[39] G. N. Agakishiyev *et al.*, Multiplicity, momentum and angular characteristics of π^- mesons for pC, dC, αC and CC interactions at 4.2 GeV/c per nucleon, Z. Phys. C **27**, 177 (1985).

[40] D. Armutlisky *et al.*, Multiplicity, Momentum and Angular Distributions of Protons from the Interactions of p, d, α and C with Carbon at 4.2 GeV/c/Nucleon Momentum, Z. Phys. A **328**, 455 (1987).

[41] A. I. Bondarenko *et al.*, The Ensemble of interactions on carbon and hydrogen nuclei obtained using the 2 m propane bubble chamber exposed to the beams of protons and H-2, He-4, C-12 relativistic nuclei at the Dubna Synchrophasotron (Dubna, 1998), JINR Preprint No. P1-98-292.

[42] V. D. Toneev, N. S. Amelin, K. K. Gudima, and S. Yu. Sivoklokov, Dynamics of relativistic heavy-ion collisions, Nucl. Phys. A **519**, 463 (1990).

[43] N. S. Amelin, K. K. Gudima, and S. Yu. Sivoklokov, and V. D. Toneev, Further Development Of A Quark-Gluon String Model For Describing High-energy Collisions With A Nuclear Target, Sov. J. Nucl. Phys. **52**, 172 (1990).

[44] N. S. Amelin, K. K. Gudima, and V. D. Toneev, Ultrarelativistic nucleus-nucleus collisions within a dynamical model of quark-gluon strings, Sov. J. Nucl. Phys. **51**, 1093 (1990).

[45] N. S. Amelin, E. F. Staubo, L. P. Csernai, V. D. Toneev, and K. K. Gudima, Strangeness production in proton and heavy ion collisions at 14.6A GeV, Phys. Rev. C **44**, 1541 (1991).

[46] M. Anikina *et al.*, The analysis of π^- mesons produced in nucleus-nucleus collisions at a momentum of 4.5 GeV/c nucleon in light front variables, Eur. Phys. J. A **7**, 139 (2000).

[47] L. Bravina *et al.*, Fluid dynamics and quark gluon string model: What we can expect for Au+Au collisions at 11.6A GeV/c, Nucl. Phys. A **566**, 461 (1994).

[48] B. Gankhuyag and V. V. Uzhinskii, Modified FRITIOF code: Negative charged particle production in high-energy nucleus-nucleus interactions (Dubna, 1996), JINR Preprint No. P2-96-419.

[49] A. S. Galoyan, G. L. Melkumov, and V. V. Uzhinskii, Analysis of charged-particle production in nucleus–nucleus interactions near and beyond the kinematical limit for free NN collisions within the FRITIOF model, Phys. Atom. Nucl. **65**, 1722 (2002).

[50] A. I. Bondarenko *et al.*, Features of CC interactions at a momentum of 4.2 GeV/c per nucleon for various degrees of nuclear collision centrality, Phys. Atom. Nucl. **65**, 90 (2002).

[51] A. S. Galoyan *et al.*, Features of pC interactions at a momentum of 4.2 GeV/c versus the degree of centrality of collisions between protons and carbon nuclei: Multiplicity of secondary particles, Phys. Atom. Nucl. **66**, 836 (2003).

[52] Ts. Baatar *et al.*, Analyzing the features of π^- mesons and protons from AC interactions at a momentum of $p = 4.2$ GeV/c per projectile nucleon on the basis of the FRITIOF model, Phys. Atom. Nucl. **63**, 839 (2000).

[53] R. Hagedorn and J. Ranft, Statistical thermodynamics of strong interactions at high-energies. 2. Momentum spectra of particles produced in pp collisions, Suppl. Nuovo Cimento **6**, 169 (1968).

[54] G. N. Agakishiev, S. Backovic, V. Boldea *et al.*, Comparative characteristics of central and noncentral CC interactions at 4.2 GeV/c per nucleon (Dubna, 1989), JINR Preprint P-1-89-488.

[55] I. Bearden *et al.* (NA44 Collaboration), Collective expansion in high energy heavy ion collisions, Phys. Rev. Lett. **78**, 2080 (1997).

[56] L. Chkhaidze, P. Danielewicz, T. Djobava, L. Kharkhelauri, and E. Kladnitskaya, Collective flow of protons and negative pions in nucleus–nucleus collisions at a momentum of $4.2 - 4.5A$ GeV/c, Nucl. Phys. A **794**, 115 (2007).

[57] L. Chkhaidze *et al.*, Collective flows of protons and π^- mesons in ^{2}H +C,Ta and He + C, Ta collisions at 3.4 GeV/nucleon, Phys. Rev. C **84**, 064915 (2011).

[58] L. V. Chkhaidze *et al.*, Study of collective flow effects in CC collisions at a momentum of 4.2 GeV/c per nucleon, Phys. Atom. Nucl. **67**, 693 (2004).

[59] A. Bialas *et al.*, Multiplicity distributions in nucleus-nucleus collisions at high-energies, Nucl. Phys. B **111**, 461 (1976).

[60] Y. M. Shabelsky, On the multiplicity of the secondaries produced in collisions of relativistic nuclei, Acta Phys. Pol. B **10**, 1049 (1979).

[61] Lj. Simic *et al.*, Dependence of average characteristics of π^- mesons on number of interacting protons in nucleus-nucleus collisions at 4.2 GeV/c per nucleon, Phys. Rev. D **34**, 692 (1986).

[62] N. Angelov *et al.*, Interaction Cross Sections and Negative pion Multiplicities in Nucleus-Nucleus Collisions at 4.2 GeV/c Per Nucleon, Sov. J. Nucl. Phys. **33**, 552 (1981).

[63] B. Bracci *et al.*, Compilations of cross sections III $- p$ and p-bar induced reactions, CERN/HERA 73–1 (CERN, 1973).

[64] B. I. Abelev *et al.* (STAR Collaboration), Systematic measurements of identified particle spectra in pp, $d +$ Au, and Au + Au collisions at the STAR detector, Phys. Rev. C **79**, 034909 (2009).

[65] F. Karsch, Lattice QCD at high temperature and density, Lect. Notes Phys. **583**, 209 (2002).

[66] L. Chkhaidze *et al.*, Study of the inclusive reaction Mg + Mg $\rightarrow$ $\pi^- + X$ at a momentum of 4.3 GeV/c per incident nucleon, J. Phys. G **22**, 641 (1996).

[67] B. Hong *et al.*, Stopping and radial flow in central ^{58}Ni + ^{58}Ni collisions between 1A and 2A GeV, Phys. Rev. C **57**, 244 (1998).

[68] A. Gilg *et al.*, GSI Scientific Report No. 96-1, Darmstadt (1996), p. 52.

[69] M. Pfeiffer *et al.*, GSI Scientific Report No. 93-1, Darmstadt (1993), p. 58.

[70] O. Schwalb *et al.*, GSI Scientific Report No. 93-1, Darmstadt (1993), p. 62.

[71] M. Appenheimer *et al.*, GSI Scientific Report No. 97-1, Darmstadt (1997), p. 58.

[72] C. Muntz *et al.*, GSI Scientific Report No. 95-1, Darmstadt (1995), p. 77.

[73] N. Herrmann, J. P. Wessels, and T. Wienold, Collective flow in heavy-ion collisions, Annu. Rev. Nucl. Part. Sci. **49**, 581 (1999).